

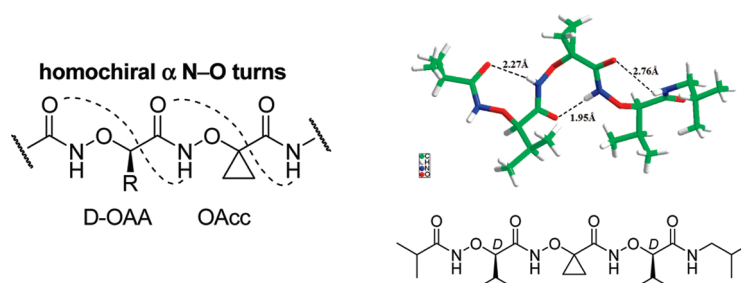
Chiral α -Aminoxy Acid/Achiral Cyclopropane α -Aminoxy Acid Unit as a Building Block for Constructing the α N–O Helix

Dan Yang,^{*,†,‡} Xiao-Wei Chang,[†] Dan-Wei Zhang,^{*,†} Ze-Feng Jiang,[‡] Ke-Sheng Song,[‡] Yu-Hui Zhang,[‡] Nian-Yong Zhu,[‡] Lin-Hong Weng,[†] and Min-Qin Chen[†]

[†]Department of Chemistry, Fudan University, Shanghai 200433, China, and [‡]Department of Chemistry, The University of Hong Kong, Pokfulam Road, Hong Kong, China

yangdan@hku.hk; zhangdw@fudan.edu.cn

Received April 28, 2010



The monomer **1** derived from achiral 1-(aminoxy)cyclopropanecarboxylic acid (OAcc) and oligopeptides **2–9** consisting of a chiral α -aminoxy acid and an achiral α -aminoxy acid such as OAcc were synthesized and their structures characterized. The eight-membered-ring intramolecular hydrogen bond, namely the α N–O turn, was formed between adjacent residues independent of their chirality. However, the helix formation was sequence-dependent. Dipeptide **2** bearing chiral α -aminoxy acid (D-OAA) at the N-terminus and achiral OAcc at the C-terminus preferentially adopted a right-handed 1.8_8 helical structure, but dipeptide **3** (OAcc-D-OAA) did not. Theoretical calculation results, in good agreement with experimental ones, revealed that the biased handedness of α N–O turn found in OAcc residue depends on its preceding chiral residue. It was then found that the helical conformation was destroyed in the case of oligopeptides **6** and **7** [OAA-(OAcc) $_n$, $n = 2, 3$]. The crystal structure of tripeptide **8** (*i*PrCO-D-OVal-OAcc-D-OVal-NH^{*t*}Bu) further disclosed the helical structure formed by three consecutive homochiral α N–O turns. This study has uncovered achiral aminoxy acid residues such as the OAcc unit as a useful building block to be incorporated into chiral aminoxy peptides to mimic chiral helix structure.

Introduction

Helices are ubiquitous in nature and play a paramount role in many biological recognition processes.¹ For their functional importance, great efforts have been dedicated to

modeling the chiral helix system in synthetic polymers.² The foldamers prepared from chiral monomers, such as β -³ and γ -amino acids,⁴ can mimic the secondary structures of natural peptides by formation of novel helices, and the intramolecular hydrogen-bonding pattern of those oligomer backbones is primarily determined by the substitution mode of the chiral building blocks. On the other hand, the incorporation of the highly constrained achiral amino acid into

(1) (a) Hecht, S.; Huc, I. *Foldamers: Structure, Properties, and Applications*; Wiley-VCH: Weinheim, 2007. (b) Champe, P. C.; Harvey, R. A.; Ferrier, D. R. *Biochemistry*, 4th ed.; Lippincott Williams & Wilkins: New York, 2007.

(2) For selected reviews, see: (a) Hecht, S.; Huc, I. *Foldamers*; Wiley-VCH: Weinheim, 2007. (b) Nakano, T.; Okamoto, Y. *Chem. Rev.* **2001**, *101*, 4013. (c) Hill, D. J.; Mio, M. J.; Prince, R. B.; Hughes, T. S.; Moore, J. S. *Chem. Rev.* **2001**, *101*, 3893. (d) Venkatraman, J.; Shankaramma, S. C.; Balaram, P. *Chem. Rev.* **2001**, *101*, 3131. (e) Gellman, S. H. *Chem. Rev.* **1998**, *31*, 173. (f) Yashima, E.; Maeda, K.; Nishimura, T. *Chem.—Eur. J.* **2004**, *10*, 42. (g) Yashima, E.; Maeda, K.; Furusho, Y. *Acc. Chem. Res.* **2008**, *41*, 1166. (h) Cornelissen, J. J. L. M.; Rowan, A. E.; Nolte, R. J. M.; Sommerdijk, N. A. J. M. *Chem. Rev.* **2001**, *101*, 4039. (i) Li, X.; Yang, D. *Chem. Commun.* **2006**, 3367.

(3) For reviews, see: (a) Cheng, R. P.; Gellman, S. H.; DeGrado, W. F. *Chem. Rev.* **2001**, *101*, 3219. (b) Seebach, D.; Beck, A. K.; Bierbaum, B. J. *Chem. Biodiversity* **2004**, *1*, 1111.

(4) For recent examples of γ -peptides, see: (a) Hubatsch, I.; Arvidsson, P. I.; Seebach, D.; Luthman, K.; Artursson, P. *J. Med. Chem.* **2007**, *50*, 5238. (b) Seebach, D.; Hook, D. F.; Glättli, A. *Biopolymers* **2006**, *84*, 23. (c) Seebach, D.; Schaeffer, L.; Brenner, M.; Hoyer, D. *Angew. Chem., Int. Ed.* **2003**, *42*, 776.

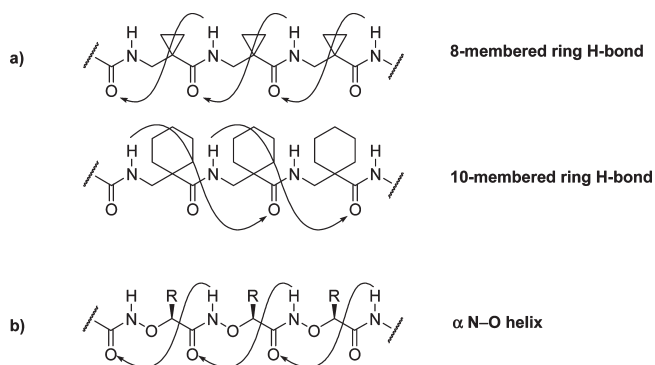


FIGURE 1. (a) Intramolecular hydrogen bonds in achiral $\beta^{2,2}$ -peptides; (b) α N–O helix in homochiral α -aminoxy peptides.

peptides would enhance or suppress the bioactivities of peptides, which are shape-dependent.⁵ This strategy can also be applied in the field of peptidomimetics. An achiral building block bearing highly constrained side chains can rigidify the backbone or create new secondary structures. For example, in the oligomers composed of $\beta^{2,2}$ -amino acid—1-(aminomethyl)cyclopropyl carboxylic acid, the 8-membered-ring intramolecular hydrogen bonds were formed,⁶ while in the oligomers derived from 1-(aminomethyl)cyclohexylcarboxylic acid,⁷ the 10-membered-ring intramolecular hydrogen bonds were observed (Figure 1a). The former mode of intramolecular hydrogen bond has not been found in the known chiral β^2 -peptides. Furthermore, the achiral residue or segment may also exhibit biased chiral conformation if incorporated into oligomers containing chiral residues,⁸ which is analogous to the behavior of achiral α -aminoisobutyric acid (Aib) in building peptides.⁹

(5) For some examples employing constrained cyclopropyl rings, see: (a) Burgess, K.; Li, W.; Lim, D.; Moye-Sherman, D. *Biopolymers* **1997**, *42*, 439. (b) Burgess, K.; Ho, K.-K.; Pettitt, B. M. *J. Am. Chem. Soc.* **1994**, *116*, 799. (c) Burgess, K.; Ho, K.-K.; Pettitt, B. M. *J. Am. Chem. Soc.* **1995**, *117*, 54. (d) Burgess, K.; Ho, K.-K.; Pal, B. *J. Am. Chem. Soc.* **1995**, *117*, 3808. (e) Burgess, K.; Ke, C.-Y. *J. Org. Chem.* **1996**, *61*, 8627.

(6) Abele, S.; Seiler, P.; Seebach, D. *Helv. Chim. Acta* **1999**, *82*, 1559. (7) Seebach, D.; Abele, S.; Sifferlen, T.; Hänggi, M.; Gruner, S.; Seiler, P. *Helv. Chim. Acta* **1998**, *81*, 2218.

(8) (a) Mazaleyrat, J.-P.; Wright, K.; Gaucher, A.; Toulemonde, N.; Wakselman, M.; Oancea, S.; Peggion, C.; Formaggio, F.; Setnička, V.; Keiderling, T. A.; Toniolo, C. *J. Am. Chem. Soc.* **2004**, *126*, 12874. (b) Mazaleyrat, J.; Wright, K.; Gaucher, A.; Toulemonde, N.; Dutot, L.; Wakselman, M.; Broxterman, Q. B.; Kaptein, B.; Oancea, S.; Peggion, C.; Crisma, M.; Formaggio, F.; Toniolo, C. *Chem.—Eur. J.* **2005**, *11*, 6921. (c) Dutot, L.; Wright, K.; Gaucher, A.; Wakselman, M.; Mazaleyrat, J.-P.; Zotti, M. D.; Peggion, C.; Formaggio, F.; Toniolo, C. *J. Am. Chem. Soc.* **2008**, *130*, 5986. (d) Formaggio, F.; Crisma, M.; Toniolo, C.; Tchernanov, L.; Guilhem, J.; Mazaleyrat, J.-P.; Gaucher, A.; Wakselman, M. *Tetrahedron* **2000**, *56*, 8721.

(9) For some examples, see: (a) Toniolo, C.; Crisma, M.; Formaggio, F.; Peggion, C. *Biopolymers* **2001**, *60*, 396. (b) Benedetti, E.; Saviano, M.; Iacovino, R.; Pedone, C.; Santini, A.; Crisma, M.; Formaggio, F.; Toniolo, C.; Broxterman, Q. B.; Kamphuis, J. *Biopolymers* **1998**, *46*, 433. (c) Formaggio, F.; Crisma, M.; Toniolo, C.; Bonora, G. M.; Broxterman, Q. B.; Kamphuis, J.; Saviano, M.; Iacovino, R.; Rossi, F.; Benedetti, E. *J. Chem. Soc., Perkin Trans. 2* **1998**, 1651. (e) Benedetti, E.; Bavoso, A.; Di Blasio, B.; Pavone, V.; Pedone, C.; Crisma, M.; Bonora, G. M.; Toniolo, C. *J. Am. Chem. Soc.* **1982**, *104*, 2437. (f) Clayden, J.; Castellanos, A.; Sol, J.; Morris, G. *Angew. Chem., Int. Ed.* **2009**, *48*, 5962.

(10) (a) Yang, D.; Qu, J.; Li, B.; Ng, F.-F.; Wang, X.-C.; Cheung, K.-K.; Wang, D.-P.; Wu, Y.-D. *J. Am. Chem. Soc.* **1999**, *121*, 589. (b) Yang, D.; Li, B.; Ng, F.-F.; Yan, Y.-L.; Qu, J.; Wu, Y.-D. *J. Org. Chem.* **2001**, *66*, 7303. (c) Wu, Y.-D.; Wang, D.-P.; Chan, K. W. K.; Yang, D. *J. Am. Chem. Soc.* **1999**, *121*, 11189. (d) Yang, D.; Li, W.; Qu, J.; Luo, S.-W.; Wu, Y.-D. *J. Am. Chem. Soc.* **2003**, *125*, 13018. (e) Yang, D.; Liu, G.-J.; Hao, Y.; Li, W.; Dong, Z.-M.; Zhang, D.-W.; Zhu, N.-Y. *Chem. Asian J.* **2010**, *5*, 1356.

Our group has previously reported the α N–O helical structure adopted by the homochiral oligopeptides of mono-substituted α -aminoxy acids (Figure 1b)¹⁰ through the formation of consecutive homochiral α N–O turns (8-membered-ring intramolecular hydrogen bond) between the C=O_(i) oxygen and the N–H_(i+2) proton.^{10a,11} The α N–O turn prevails in those oligopeptides, in which the left-handed α N–O turn is adopted by the L-aminoxy acid residue and the right-handed one adopted by the D-aminoxy acid residue.^{10a,b,12} The independence of the α N–O turn on the side chain of the α -aminoxy acid residue has been well-documented.¹⁰ The α N–O helix or reverse turn structure can be easily constructed in the homochiral or heterochiral α -aminoxy dipeptides, respectively. An interesting question which follows is whether the introduction of a rigid cyclopropyl ring to construct the achiral disubstituted α -aminoxy acid [1-(aminoxy)cyclopropanecarboxylic acid, OAcc] would lead to any variation in the conformation. In an effort to explore the conformational characteristic of OAcc and its performance in building α N–O helix with other chiral aminoxy acid residues, we have synthesized the OAcc monomer and oligopeptides consisting of OAcc and chiral OAA residues and studied their secondary structures by multiple analytical methods. The detailed results are disclosed below.

Results and Discussion

Synthesis of OAcc Monomer 1 and the Structures of Oligopeptides 2–9. We prepared monomer **1**, which is derived from achiral 1-(aminoxy)cyclopropanecarboxylic acid (OAcc), oligopeptides **2**, **3**, and **6–9** bearing chiral α -aminoxy acid OAA and achiral α -aminoxy acid OAcc, and oligopeptides **4** and **5** bearing OAA and achiral 2-aminoxyacetic acid (OGly) for conformational studies (Chart 1).¹³ The synthesis of fully protected OAcc employed serine as the starting material (Scheme 1). The key intermediate 2-phthalylaminoxy acrylate methyl ester (**11**) was obtained by dehydration of the N-terminally protected OSer. It then underwent 1,3-dipolar cycloaddition with diazomethane to afford PhthN-OAcc-OMe (**12**) upon heating. The amide bond was constructed by conventional coupling method.

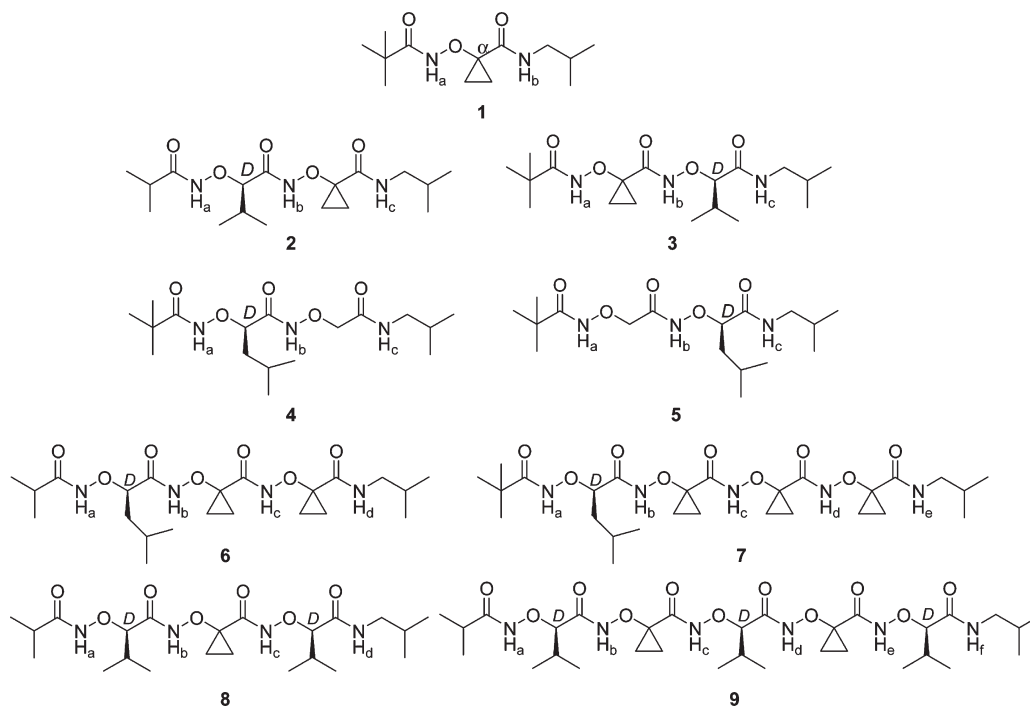
The synthesis of oligopeptides **2–9** followed the conventional peptide coupling method starting from N- and C-terminally protected aminoxy acids.¹³

Conformation of OAcc Monomer: Compound 1. The conformation of compound **1** in solution¹³ was studied by ¹H NMR dilution and titration experiments, combined with FT-IR characterization (Figure 2). Amide proton NH_b of compound **1** proved to be intramolecularly hydrogen-bonded, for its chemical shift (8.65 ppm) at low concentration (ca. 2 mM in CDCl₃) was more downfield than that of the regular amide proton, and it remained virtually unchanged upon dilution with CDCl₃ or titration with DMSO-*d*₆.¹¹ In contrast, the aminoxy amide proton NH_a of compound **1** was not intramolecularly hydrogen-bonded, for its chemical shift moved downfield dramatically in these two experiments.¹³

According to previous FT-IR studies of aminoxy acid oligomers,¹¹ the bands at 3394 and 3307 cm⁻¹ could be

(11) Yang, D.; Ng, F.-F.; Li, Z.-J. *J. Am. Chem. Soc.* **1996**, *118*, 9794. (12) (a) Yang, D.; Qu, J.; Li, W.; Wang, D.-P.; Ren, Y.; Wu, Y.-D. *J. Am. Chem. Soc.* **2003**, *125*, 14452. (b) Yang, D.; Qu, J.; Li, W.; Zhang, Y.-H.; Ren, Y.; Wang, D.-P.; Wu, Y.-D. *J. Am. Chem. Soc.* **2002**, *124*, 12410. (13) For details, see the Supporting Information.

CHART 1



SCHEME 1. Synthesis of Compound 1 Starting from L-Serine

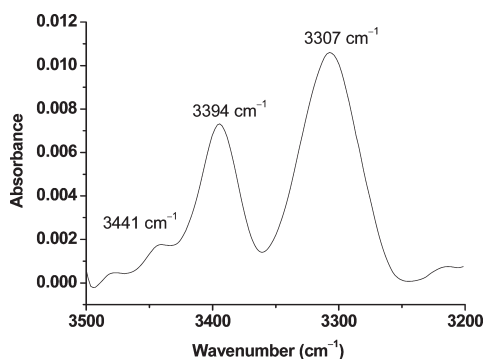
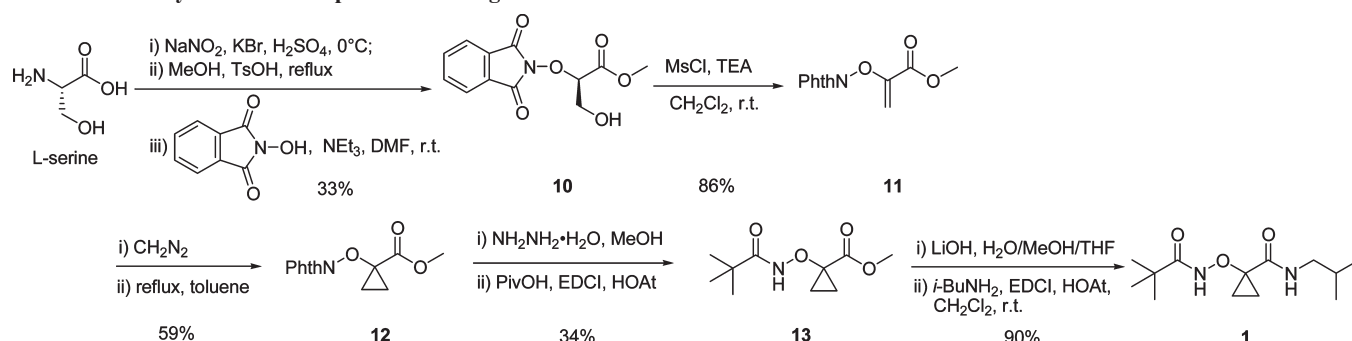


FIGURE 2. N–H stretching region of FT-IR spectra for compounds **1** at 2 mM in CH_2Cl_2 at room temperature after subtraction of the spectrum of pure CH_2Cl_2 .

assigned to the stretching of non-hydrogen-bonded *N*-oxy amide N–H_a and hydrogen-bonded regular amide N–H_b, respectively (Figure 2). The stretch band of non-hydrogen-bonded regular amide N–H_b was almost undetectable, for

the peak around 3441 cm^{-1} was even smaller than the corresponding OGly monomer reported previously.¹¹ Current evidence strongly suggests that compound **1** formed the eight-membered-ring intramolecular hydrogen bond between the *C*-terminal regular amide NH_b and the *N*-terminal carbonyl oxygen almost exclusively in solution.

The single crystal of compound **1** was obtained for the characterization of its structure in the solid state (Figure 3). A twinned crystal structure was found for compound **1**.¹³ As expected, compound **1** exists as a pair of mirror image structures with dihedral angles of the same values but opposite signs. The hyperconjugative overlap between the carbonyl π bond and the cyclopropane C–C bond fixes the O–C_α and C=O bonds of OAcc residue anti to each other, with the C=O bond bisecting the cyclopropyl ring.¹⁴

Formation of the α N–O Turn with Biased Handedness in the OAcc (OGly) Residue of Dipeptides 2–5. Based on the rigid α N–O turn structure in the OAcc monomer,

(14) Zhao, H. *Drug Discovery Today* **2007**, *12*, 149.

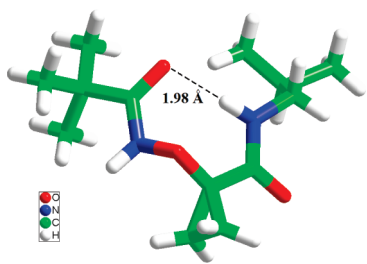


FIGURE 3. Intramolecular hydrogen bond in the crystal structure of compound **1**.

TABLE 1. ^1H NMR Chemical Shifts (δ ppm) of NH Protons of Oligopeptides **2–9** at Low Concentrations (1.56–5 mM in CDCl_3)^a

compd	NH_a	NH_b	NH_c	NH_d	NH_e	NH_f
2	8.43	11.88	<i>8.51</i>			
3	8.35	12.13	<i>8.24</i>			
4	8.36	11.81	<i>8.13</i>			
5	8.53	11.87	<i>7.90</i>			
6	8.67	12.10, 11.98		8.62		
7	8.53	12.21, 12.18, 12.17			8.59	
8	8.43	12.11, 11.93		8.38		
9	8.56	12.29, 12.27, 12.26, 12.06				8.38

^aThe chemical shifts shown in italics are those of the C-terminal regular amide NH protons; the others are those of the aminoxy amide NH protons.

dipeptides **2–5** were designed to investigate the conformational propensity of achiral aminoxy residues, OAcc and OGly, in α -aminoxy acid oligomers. Dipeptides **2** (PivCO-D-OVal-OAcc-NH^tBu) and **3** (Piv-OAcc-D-OVal-NH^tBu) consist of chiral D-OVal and rigid OAcc residues, while dipeptides **4** (Piv-D-OLeu-OGly-NH^tBu) and **5** (Piv-OGly-D-OLeu-NH^tBu) are composed of chiral D-OLeu and more flexible OGly residues.

The chemical shifts of NHs in dipeptides **2–5** were recorded at low concentrations (1.56–5 mM) in CDCl_3 (Table 1). As expected, the profiles of chemical shifts of NHs in all dipeptides were identical, which is consistent with our previous results for chiral dipeptides.^{12a} NH_b 's and NH_c 's of these four dipeptides gave significantly downfield signals, which could be assigned to the hydrogen-bonded aminoxy amide NHs and the hydrogen-bonded regular amide NHs, respectively. It is noteworthy that the chemical shifts of NHs that form the α N–O turn in the OAcc residue are more downfield than the corresponding ones in the chiral α -aminoxy acid or OGly residue.

In their FT-IR spectra (Figure 4), the hydrogen-bonded aminoxy amide NHs and regular amide NHs could be assigned unambiguously for the four dipeptides. The band at 3358 cm^{-1} for dipeptide **2**, 3392 cm^{-1} for dipeptide **3**, and 3380 cm^{-1} for dipeptides **4** and **5** were assigned to the non-hydrogen-bonded aminoxy amide N–H stretching, whereas the bands at 3328 , 3311 , 3309 , and 3334 cm^{-1} for dipeptides **2–5**, respectively, were assigned to the stretching band of the hydrogen-bonded *N*-isobutyl amide N–H_c. The absorptions in the region of $3300\text{--}3100\text{ cm}^{-1}$ were assigned to an intramolecularly hydrogen-bonded amide N–H_b stretching (3168 cm^{-1} for dipeptide **2** and dipeptide **5**, 3165 cm^{-1} for dipeptide **3**, and 3164 cm^{-1} for dipeptide **4**). However, the stretching frequencies of N–H bond are not informative of the difference among OAcc, OGly, and chiral OAA residues due to the broadness and overlap of peaks. In the region correspond-

ing to the non-hydrogen-bonded regular amide N–H (above 3400 cm^{-1}), these dipeptides showed very weak signals except for that of **4**. This means that NH_c formed an intramolecular hydrogen bond almost exclusively in OAcc, D-OVal, and D-OLeu residues.

The α N–O helical conformation, which is facilitated by consecutive homochiral α N–O turns, could be detected by circular dichroism spectroscopy. A typical right-handed α N–O helix exhibits the Cotton effect of a positive maximum at 195 nm and a negative maximum at $\sim 220\text{ nm}$.^{10a} It is noteworthy that the intensity of the CD signal for the α N–O helix is directly proportional to the number of α N–O turns formed in the homochiral α -aminoxy acid oligomers (that is, one right-handed α N–O turn contributes a positive peak at 195 nm with an intensity of $\sim 50000\text{ deg}\cdot\text{cm}\cdot\text{dmol}^{-1}$). Therefore, the CD technique provides a precise measure to indicate the number of α N–O turns in helical aminoxy oligomers. As the results of IR and ^1H NMR analysis have proved that an OAcc or OGly residue in **2–5** could form an α N–O turn as the corresponding monomer does in solution, the typical CD absorption, characteristic of an α N–O helix, will be expected for these four dipeptides if the achiral residue adopts an α N–O turn of the same handedness as the adjacent chiral residue. If the achiral residue adopts α N–O turn of opposite handedness, the CD spectra would differ. The CD spectra of **2–5** recorded in 2,2,2-trifluoroethanol (TFE) at 0.4 mM without normalization by their N–O turn numbers are shown in Figure 5. Interestingly, dipeptide **2**, whose achiral residue OAcc is located at the C-terminus, presented a curve resembling a typical α N–O helix, which indicates two consecutive right-handed α N–O turns formed in the backbone. In contrast, for dipeptide **4** consisting of an OGly-D-OLeu unit, the intensity of $\sim 60000\text{ deg}\cdot\text{cm}\cdot\text{dmol}^{-1}$ could not account for two right-handed N–O turns while it exceeded the intensity for one right-handed N–O turn. This means that only part of the dipeptide **4** possesses an α N–O helix conformation in solution. In addition, the position of the achiral residue affects the conformation of the backbone. The CD intensity of dipeptides **3** and **5** was weaker than that of **2** and **4**, respectively. The former two with chiral residue located at the C-terminus exhibited a maximum of less than $40000\text{ deg}\cdot\text{cm}\cdot\text{dmol}^{-1}$ at 195 nm without normalization by N–O turn numbers. Based on the above evidence, we conclude that this helical-sense predominance is more biased in OAcc-containing dipeptides than in OGly-containing dipeptides and that a chiral residue induces the chiral α N–O turn of OAcc or OGly more effectively when it is positioned at the N-terminus.

Why does the relative position of the achiral/chiral residue have such an impact on the backbone conformation of aminoxy dipeptides **2–5**, and why is the side chain of α,α -disubstituted aminoxy acid pertinent to the α helical fraction? To tackle these questions, DFT calculations¹⁵ were carried out on the model dipeptides Ac-L-OAla-OAcc-NHMe (**I**, Figure 6a) and Ac-OAcc-L-OAla-NHMe (**II**, Figure 6b). In both model dipeptides, L-OAla with an α carbon of *S*-configuration would lead to the formation of a left-handed α N–O turn. If the left-handedness is transmitted to the achiral OAcc residue, the dipeptide folds into a helical structure (conformers **Ia** and **IIa**). Similarly, a reverse turn structure arises if a right-handed α N–O turn is formed in the OAcc residue (conformers **Ib** and **IIb**). According to

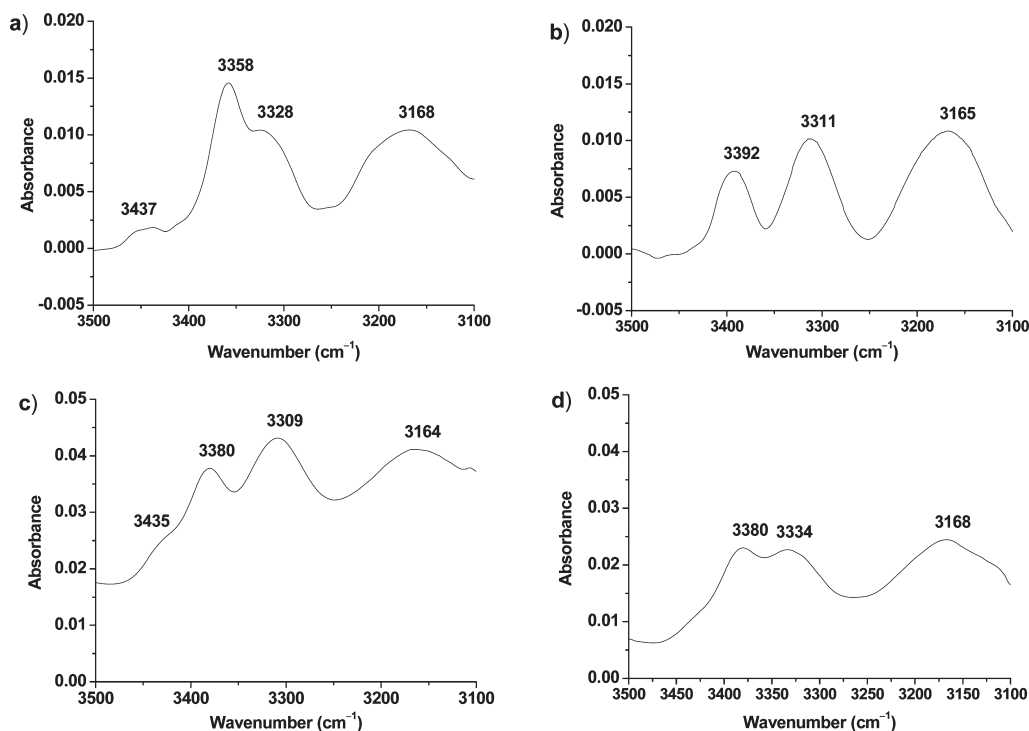


FIGURE 4. N–H stretching region of FT-IR spectra for dipeptides (a) **2**, (b) **3**, (c) **4**, and (d) **5** (2 mM in CH_2Cl_2 at room temperature after subtraction of the spectrum of pure CH_2Cl_2).

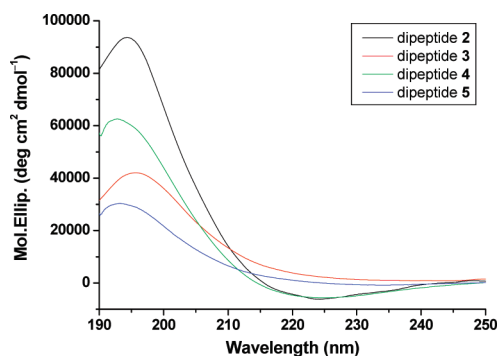


FIGURE 5. Circular dichroism (CD) spectra of dipeptides **2–5** at 0.4 mM concentration in TFE (not normalized by N–O turn numbers).

their relative energy shown in Figure 6, conformer **Ia** is more favorable than conformer **Ib**, whereas conformer **IIa** is almost equally stable to conformer **IIb** in gas phase. Consistent with this same order, the energy difference between **IIa** and **IIb** is not as significant as that between **Ia** and **Ib**

in CH_2Cl_2 . These calculation results agree well with the aforementioned experimental results.

Since the hydrogen-bond donor of the α N–O turn formed in OAcc residue is a regular amide NH in model **I** but an aminoxy amide NH in model **II**, the lowest energy conformation of Ac-OAcc-NHMe (model **III**)¹⁶ and Ac-OAcc-NHOMe (model **IV**)¹⁵ was also calculated for structural characterization (Figure 6c,d).¹³ The most stable conformer **IVa** of model **IV** bears an aminoxy NH as a hydrogen bond donor, whose intramolecular hydrogen bond is shorter in length compared with **IIIa**, the lowest energy conformation of model **III**. The bisecting conformation prevailing in the cyclopropylcarbonyl compound was distorted in model **IV**. In Table 2, the values of some dihedral angles of the OAcc unit in the lowest energy conformation of **I–IV** are summarized. For models **Ia**, **Ib**, and **IIIa**, in which the α N–O turn formed in OAcc residue is stabilized by a regular amide NH, there is no marked difference in the dihedral angles except for their sign. This highly rigid backbone in the OAcc residue gave rise to steric repulsion in the reverse-turn model **Ib**,

(15) Gaussian 98, Revision A.11.3: Frisch, M. J.; Trucks, G. W.; Schlegel, H. B.; Scuseria, G. E.; Robb, M. A.; Cheeseman, J. R.; Zakrzewski, V. G.; Montgomery, J. A., Jr.; Stratmann, R. E.; Burant, J. C.; Dapprich, S.; Millam, J. M.; Daniels, A. D.; Kudin, K. N.; Strain, M. C.; Farkas, O.; Tomasi, J.; Barone, V.; Cossi, M.; Cammi, R.; Mennucci, B.; Pomelli, C.; Adamo, C.; Clifford, S.; Ochterski, J.; Petersson, G. A.; Ayala, P. Y.; Cui, Q.; Morokuma, K.; Salvador, P.; Dannenberg, J. J.; Malick, D. K.; Rabuck, A. D.; Raghavachari, K.; Foresman, J. B.; Cioslowski, J.; Ortiz, J. V.; Baboul, A. G.; Stefanov, B. B.; Liu, G.; Liashenko, A.; Piskorz, P.; Komaromi, I.; Gomperts, R.; Martin, R. L.; Fox, D. J.; Keith, T.; Al-Laham, M. A.; Peng, C. Y.; Nanayakkara, A.; Challacombe, M.; Gill, P. M. W.; Johnson, B. G.; Chen, W.; Wong, M. W.; Andres, J. L.; Gonzalez, C.; Head-Gordon, M.; Replogle, E. S.; Pople, J. A. Gaussian, Inc., Pittsburgh, PA, 2001.

(16) Gaussian 03, Revision C.02: Frisch, M. J.; Trucks, G. W.; Schlegel, H. B.; Scuseria, G. E.; Robb, M. A.; Cheeseman, J. R.; Montgomery, J. A., Jr.; Vreven, T.; Kudin, K. N.; Burant, J. C.; Millam, J. M.; Iyengar, S. S.; Tomasi, J.; Barone, V.; Mennucci, B.; Cossi, M.; Scalmani, G.; Rega, N.; Petersson, G. A.; Nakatsuji, H.; Hada, M.; Ehara, M.; Toyota, K.; Fukuda, R.; Hasegawa, J.; Ishida, M.; Nakajima, T.; Honda, Y.; Kitao, O.; Nakai, H.; Klene, M.; Li, X.; Knox, J. E.; Hratchian, H. P.; Cross, J. B.; Bakken, V.; Adamo, C.; Jaramillo, J.; Gomperts, R.; Stratmann, R. E.; Yazyev, O.; Austin, A. J.; Cammi, R.; Pomelli, C.; Ochterski, J. W.; Ayala, P. Y.; Morokuma, K.; Voth, G. A.; Salvador, P.; Dannenberg, J. J.; Zakrzewski, V. G.; Dapprich, S.; Daniels, A. D.; Strain, M. C.; Farkas, O.; Malick, D. K.; Rabuck, A. D.; Raghavachari, K.; Foresman, J. B.; Ortiz, J. V.; Cui, Q.; Baboul, A. G.; Clifford, S.; Cioslowski, J.; Stefanov, B. B.; Liu, G.; Liashenko, A.; Piskorz, P.; Komaromi, I.; Martin, R. L.; Fox, D. J.; Keith, T.; Al-Laham, M. A.; Peng, C. Y.; Nanayakkara, A.; Challacombe, M.; Gill, P. M. W.; Johnson, B.; Chen, W.; Wong, M. W.; Gonzalez, C.; Pople, J. A. Gaussian, Inc., Wallingford, CT, 2004.

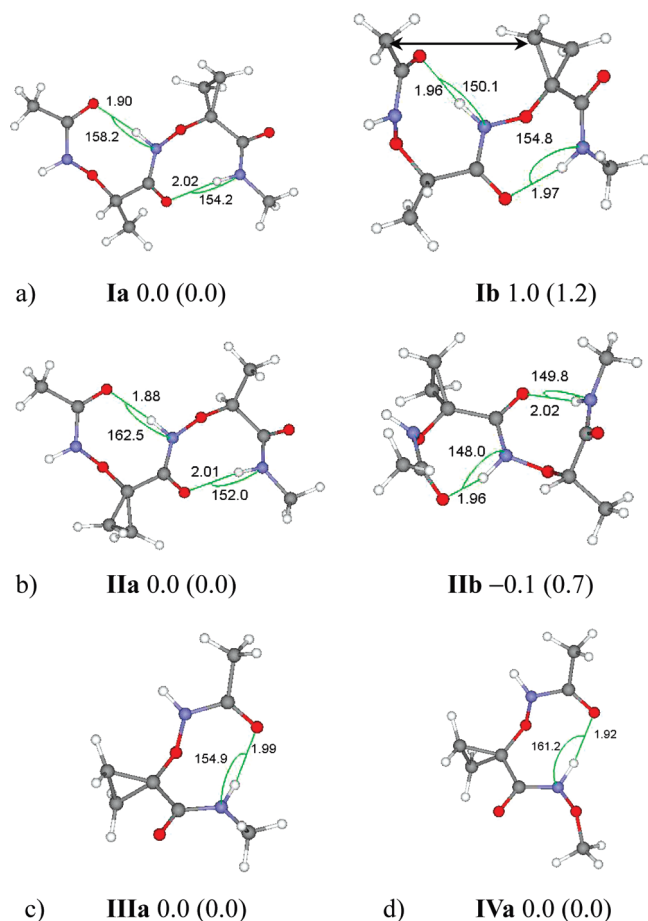


FIGURE 6. Calculated structures of (a) Ac-L-OAla-OAcc-NHMe (**I**), (b) Ac-OAcc-L-OAla-NHMe (**II**), (c) Ac-OAcc-NHMe (**III**), and (d) Ac-OAcc-NHOMe (**IV**) and their relative energies at the MP2/6-311+G** level in vacuum and in CH₂Cl₂ (in parentheses).

which occurred between the methylene group of OAcc and the N-terminal acetyl group (Figure 6a, right). This may account for the much lower stability of the reverse turn for model **I**. For comparison of the dihedral angles of models **IIa**, **IIb**, and **IV**, ψ in **IIb** is apparently smaller in value than that of the other two and is close to that of **IIIa** (**Ia**, **Ib**). The dihedral angle $\angle C'C_{\alpha}C=O$ in **IIb** is closer to 30° than that in **IIa** and **IV**. This suggests that the most stable bisecting conformation for cyclopropylcarbonyl compound is restored in **IIb**. Meanwhile, there is no inherent steric interaction between any atom or group in model **IIb**. It is therefore reasonable to assume that the energy barrier between the α N–O helix and reverse turn is not so significant in model dipeptide **II** as in model **I**. It also explains why the discrimination of helix in dipeptide **3** in TFE is much weakened compared with dipeptide **2**. This chiral induction effect is contrary to that of dipeptides based on Bip (2',1':1,2;1'',2'':3,4-dibenzcyclohepta-1,3-diene-6-amino-6-carboxylic acid)/D-Val, in which chiral induction takes place when a chiral residue is located at the C-terminus.^{8a}

On the basis of the above interpretations, it can be postulated that OGly-based dipeptide **4** would not induce steric interaction in its reverse turn conformer as does dipeptide **2** because the OGly residue bears no substituent on α -carbon. This corresponds to a low energy difference

TABLE 2. Dihedral Angle Values of $\angle C'C_{\alpha}C=O$, ϕ , θ , and ψ of the OAcc Residue in the Calculated Structures of Models I–IV

dihedral angle (deg)	Ia	Ib	IIIa	IIa	IIb	IVa
$\angle C'C_{\alpha}C=O$	25.9	25.2	24.4	21.7	27.9	21.6
ϕ	123.3	-118.2	123.4	119.3	-124.4	121.4
θ	-85.5	85.4	-83.3	-86.8	82.6	-83.8
ψ	-3.9	4.1	-5.3	-10.2	-0.8	-11.4

between the helix conformer and its reverse-turn counterpart of dipeptide **4**, and thus low CD intensity has been detected.

Different Secondary Structures of the Oligomers with the OAcc Residue Elongated on the C-Terminus of D-OAA-OAcc Dipeptide and the Oligomers Comprising Alternating D-OAA/OAcc Residues. From the above results, we have confirmed that the α N–O helix fraction is higher in the OAA–OAcc segment than in the OAA–OGly segment and that the preceding α D-aminoxy acid residue would lead to a right-handed α N–O turn of its adjacent achiral OAcc residue to the largest extent. The next logical question to be resolved is how this helical chirality is propagated along the elongated OAcc chain at the C-terminus by studying the conformation of tripeptide **6** and tetrapeptide **7**. In addition, conformational studies of tripeptide **8** and pentapeptide **9** can provide insight as to whether a chiral aminoxy residue would exert a negative effect on the chiral α N–O turn formed in its preceding OAcc residue.

As shown in Table 1, tripeptides **6** and **8**, tetrapeptide **7**, and pentapeptide **9** gave relatively downfield signals for all NH protons, assigned to hydrogen-bonded ones, except the N-terminal NH_a protons. This signal profile is highly correlated with that of dipeptides **2**–**5**. It proves that each residue in these oligomers forms an α N–O turn as expected.

As illustrated in Figure 7a, the intensities of the CD spectra of tripeptide **6** and tetrapeptide **7** were found to be the same or even slightly reduced compared with that of dipeptide **2**.¹³ This CD pattern suggests that the OAcc residues in **6** and **7** do not form a right-handed α N–O turn to a maximum extent, which means that the chirality was not propagated to the second or third achiral OAcc residue. For tetrapeptide **7**, the CD intensity even became weaker, presumably because of the increased probability of stable conformations with increasing number of residues. It is not uncommon that the helical conformation is destroyed in the longer achiral backbone. For the oligomeric groups derived from *m*-phenylenediamine, the chiral sulfinyl group or amide group could induce a chiral helix but the transmission of the chirality faded away as the backbone elongated.¹⁷

Since the OAcc residue inherits α N–O turn handedness from its immediate preceding residue, the handedness of the α N–O turn of the (*i*+1)th OAcc will be mainly determined by the *i*th OAcc. It is easy to understand that the incomplete chiral induction in *i*th OAcc, even if it were tiny, would be amplified in the (*i*+1)th OAcc and (*i*+2)th OAcc. There is another example of the OAcc oligomer analogue, namely,

(17) Clayden, J.; Lemiègre, L.; Marris, G. A.; Pickworth, M.; Snape, T. J.; Jones, L. H. *J. Am. Chem. Soc.* **2008**, *130*, 15193.

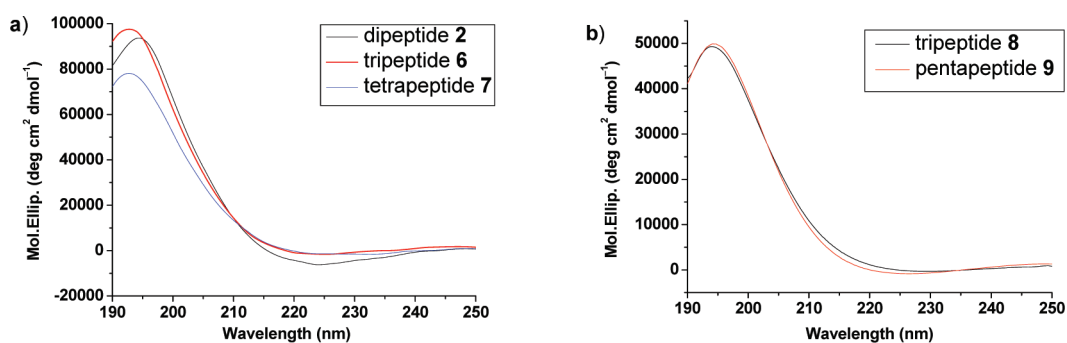


FIGURE 7. CD spectra of (a) compounds **2**, **6**, and **7** (normalized only for their concentration at 0.4 mM in trifluoroethanol) and (b) compounds **8** and **9** (normalized for their concentration at 0.4 mM in trifluoroethanol and their number of N–O turns).

the achiral β -peptides consisting of 1-(aminomethyl)cyclopropanecarboxylic acid ($\beta^{2,2}$ -Acc). Random ribbon instead of helix has been found in its crystal structure.⁶ For the high similarity of structural features between $\beta^{2,2}$ -Acc and OAcc, it has been postulated that neither $\beta^{2,2}$ -Acc nor OAcc is a helicogenic residue like OAib/ Δ Phe.^{9a,18} Thus, the transmission of α N–O turn chirality is limited in several residues.

Collectively, based on the results presented above, we know that OAA–OAcc can be regarded as an α N–O helical motif, and in principle, the more the OAA–OAcc segments are inserted, the longer the α N–O helix is constructed. Would the D-OAA residue disrupt the helical structure formed in its preceding D-OAA–OAcc segment? As shown in Figure 7b, the CD intensities of compounds **8** and **9** in TFE, normalized for their concentration and their number of N–O turns, were identical to one fully formed right-handed α N–O turn.^{10a,13} This result suggests that compounds **8** and **9** adopt a homochiral secondary structure, i.e., a right-handed α N–O helix attributed to three and five homochiral α N–O turns, respectively.¹⁹ D-OAA–OAcc would adopt a helical structure, whether it is located at the N-terminus or an intermediate position within the backbone. The immediately contiguous D- α -aminoxy acid residue would not disrupt this helical structure. D-OAA–OAcc turns out to be a very rigid right-handed α N–O helical motif which can be incorporated into aminoxy oligopeptides to build the desired secondary structures.

Hydrogen-Bonding Geometry of Dipeptide 2 and Tripeptide 8 Studied by X-ray Crystallography. In solution, dipeptide **2** adopts a helical structure as supported by evidence from CD analysis, which is also consistent with our theoretically calculated results. Nevertheless, the crystal structure of dipeptide **2** shows a typical reverse-turn structure (Figure 8a).^{12a} This discrepancy between crystal structure and solution structure has been observed in β^3 -aminoxy peptides.²⁰ The torsion angles in this crystal structure were almost identical with those in the calculated conformer **1b**.¹³ The crystal structure of dipeptide **2** was stabilized by intermolecular hydrogen bonds formed by the

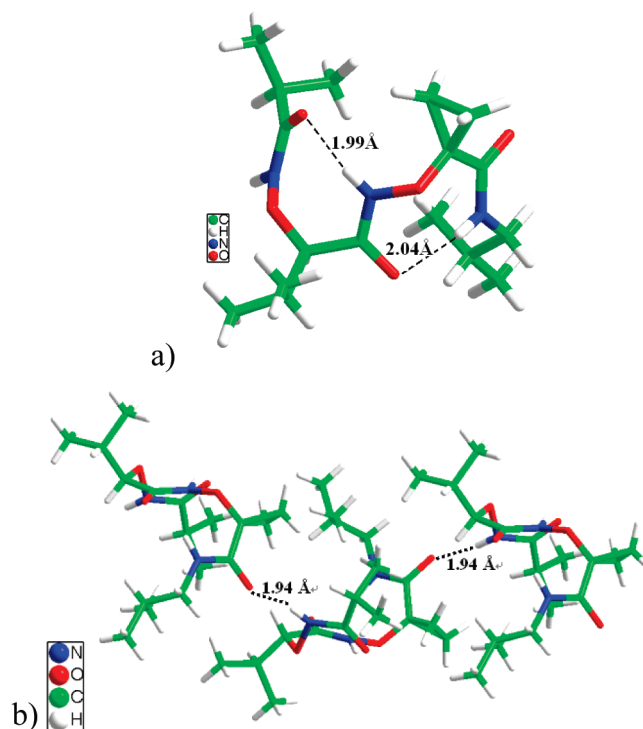


FIGURE 8. (a) Intramolecular H-bond. (b) Molecular packing in the crystal of dipeptide **2**.

aminoxy NH of OVal and the carbonyl group of OAcc in the neighboring molecule, with a very short bond length of 1.94 Å (Figure 8b). The fact that intramolecular hydrogen bonds in the crystal of **2** are longer than those in model **1b** implies that the structure of dipeptide **2** in the solid state is less crowded than **1b**, whose offset instability is caused by steric interactions to some extent.

Tripeptide **8** exhibits a helical conformation in the solid state (Figure 9a) as in solution. However, the terminal residues adopt a twisted conformation different from ordinary α N–O turn (Table 3); this is particularly true for C-terminal D-OVal with apparently larger θ (121.2°). The C $_{\alpha}$ –H bond is parallel, instead of gauche, to the N–O bond (\angle NOC $_{\alpha}$ H = 4.0°) in the C-terminal D-OVal.

The conformational change of the OVal residue may arise from the intermolecular hydrogen bonds ($d = 2.00$ Å, \angle OHN = 155.0°) formed by the aminoxy amide NH proton of the N-terminal OVal residue with the carbonyl oxygen of

(18) (a) Inai, Y.; Oshikawa, T.; Yamashita, M.; Hirabayashi, T.; Ashitaka, S. *J. Chem. Soc., Perkin Trans. 2* **2001**, 2, 892. (b) Alemán, C. *J. Phys. Chem. B* **1997**, 101, 5046. (c) Inai, Y.; Oshikawa, T.; Yamashita, M.; Tagawa, K.; Hirabayashi, T. *Biopolymers* **2003**, 70, 310. (d) Maekawa, H.; Formaggio, F.; Toniolo, C.; Ge, N.-H. *J. Am. Chem. Soc.* **2008**, 130, 6556. (e) Toniolo, C.; Benedetti, E. *Macromolecules* **1991**, 24, 4004.

(19) Compounds **2**, **3**, and **6–9** show a similar trend in the CD spectra in MeOH. See the Supporting Information for detailed information.

(20) Yang, D.; Zhang, Y.-H.; Li, B.; Zhang, D.-W.; Chan, J. C.-Y.; Zhu, N.-Y.; Luo, S.-W.; Wu, Y.-D. *J. Am. Chem. Soc.* **2004**, 126, 6956.

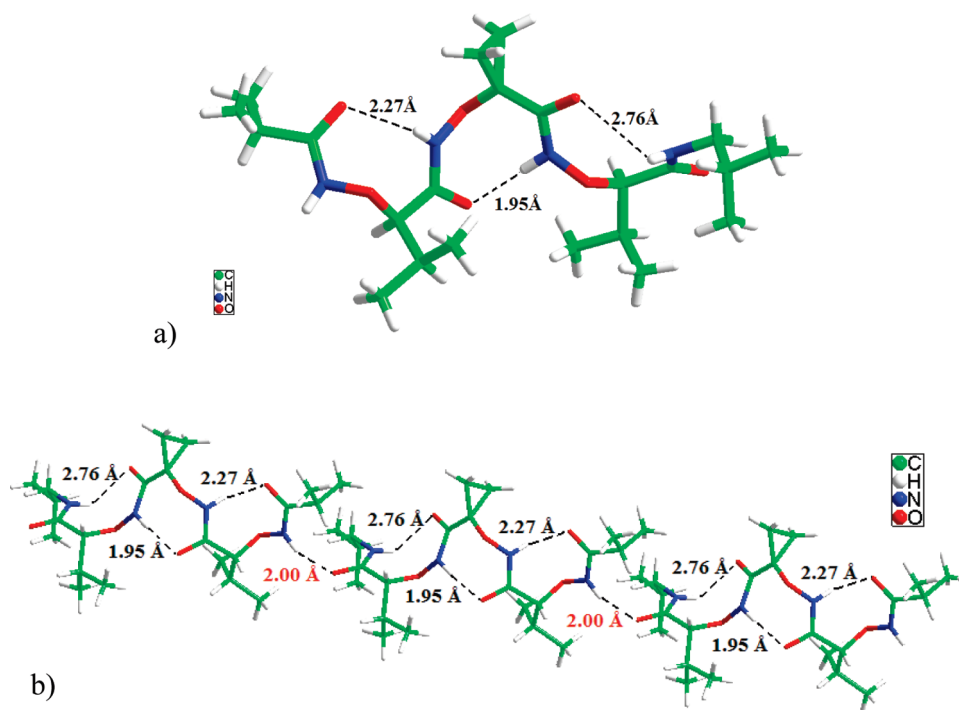


FIGURE 9. (a) Intramolecular H-bond. (b) Molecular packing in the crystal of tripeptide **8**.

TABLE 3. Intramolecular H-Bond Length (Å) and Dihedral Angle Values (deg) of the Backbone of Tripeptide **8**

	$D_{O\dots HN}$ (Å)	$\angle OHN$ (deg)	ϕ (deg)	θ (deg)	ψ (deg)
<i>N</i> -terminal OVal	2.27	126.6	-114.8	108.2	-1.0
OAcc	1.95	170.1	-121.5	79.3	12.7
<i>C</i> -terminal OVal	2.76	109.8	-113.6	121.2	-2.6

C-terminal OVal residue on the neighboring molecule (Figure 9b). It was speculated that the intermolecular hydrogen bond causes the terminal CONH plane to be twisted, elongating the intramolecular hydrogen bond in both *N*- and *C*-terminal residues. In terms of all dihedral angles related to the backbone conformation, θ is considered most labile because ϕ is determined by the rigid N–O lone-pair electron repulsion and ψ is constrained within a relatively small range by the five-membered-ring hydrogen bond formed in the *i*th aminoxy oxygen and (*i*+1)th NH. Therefore, in the solid state, tripeptide **8** forms an intermolecular hydrogen bond to pack in a compact queue by sacrificing its dihedral angle θ . Despite this twisted conformation of chiral residues, the dihedral angle θ of OAcc has the same sign as that of the chiral residues and its conformation is less changeable (Table 3). The consistency between the solid structure and solution structure of tripeptide **8** reflects a strong handedness bias of α N–O turn in the OAcc residue, when it is positioned amid homochiral aminoxy residues.

Conclusion

A helical structure has been for the first time discovered in aminoxy oligomers comprising a chiral aminoxy acid residue and an achiral OAcc residue. Together with insights from theoretical calculations, it is revealed that steric interaction between the cyclopropane methylene group and *N*-terminal group is responsible for the biased handedness of the α N–O

turn in the OAcc residue. We found that the helical conformation is destroyed with the OAcc residue elongated at the *C*-terminus of the OAA–OAcc segment, though it would not be disrupted by its subsequent chiral OAA residue. Dipeptide **2** has a reverse-turn structure, while tripeptide **8** assumes a distorted helical conformation in the solid state. The structural variations of these compounds in the solid state can be ascribed to the underlying forces that determine molecular packing, e.g., intermolecular hydrogen bond. In the crystal structures of the three compounds reported herein, the OAcc residue shows an almost identical conformation.

In view of these observations, the highly constrained OAcc residue is proved to be a promising candidate in building a rigid α N–O turn. It could be placed at the *C*-terminus or inserted into homochiral α aminoxy peptides to form an α N–O turn with biased handedness. This study advanced a new understanding about the profound nature of aminoxy acid structural characteristics and demonstrated the potential of the OAA–OAcc unit as a useful α N–O helical building block which could be incorporated into aminoxy oligopeptides to build the desired secondary structures.

Experimental Section

The oligopeptides **2–9** were prepared from α -aminoxy acid monomers with *C*- and *N*-terminal protecting groups, such as an *N*-phthaloyl group and *tert*-butyl group, following the conventional peptide coupling method.¹³ The representative experimental procedure for the coupling steps is as indicated below.

Deprotection of the *N*-Phthaloyl Group of Protected Aminoxy Acid (or Oligopeptide) with Hydrazine Hydrate¹¹. To a solution of *N*-phthaloyl-protected aminoxy acid (or oligopeptide) (3.00 mmol) in anhydrous methanol (10 mL) was added hydrazine hydrate (0.62 mL, 9 mmol). The resulting reaction mixture was stirred at room temperature for 1 h. After the reaction mixture

was concentrated under vacuum, 3% sodium carbonate solution (10 mL) was added. The resultant solution was then extracted with ether (3 × 20 mL), and the combined organic layer was dried over anhydrous sodium sulfate and concentrated to afford the crude product, which was directly used in the next step.

Deprotection of the *C*-*tert*-Butyl Group of Protected Aminoxy Acid (or Oligopeptide) with 2,2,2-Trifluoroacetic Acid (TFA)¹¹. A solution of *C*-*tert*-butyl-protected aminoxy acid (or oligopeptide) (1.73 mmol) in dichloromethane (5 mL) in an ice bath was treated with trifluoroacetic acid (5 mL). After being stirred at room temperature for 1 h, the reaction mixture was concentrated under vacuum and azeotroped with toluene. The crude product thus obtained was directly used in the next step.

Deprotection of the *C*-Methyl Group of the Protected Aminoxy Acid (or Oligopeptide) with LiOH/THF/H₂O. To a solution of *C*-methyl-protected aminoxy acid (or oligopeptide) (1.5 mmol) in THF (8 mL) and water (1 mL) was added LiOH (190 mg, 4.5 mmol). The reaction mixture was stirred at room temperature for 2 h. When the reaction was complete as monitored by TLC, the mixture was concentrated and then diluted with deionized water (5 mL). The resultant aqueous solution was then acidified with 10% HCl aqueous solution to pH ~2, followed by extraction with ethyl acetate (15 mL × 2). The combined organic layer was dried over anhydrous MgSO₄ and concentrated to afford the crude product, which was directly used in the next step.

Coupling of *N*-Deprotected Aminoxy Acid (or Oligopeptide) with Isobutyric Acid or Pivalic Acid. Isobutyric acid or pivalic acid (3 mmol) was added to a solution of *N*-deprotected aminoxy acid (or oligopeptide) in CH₂Cl₂ (10 mL). To this mixture were added HOAt (612 mg, 4.50 mmol) and EDCI (891 mg, 3 mmol). The reaction mixture was stirred overnight. When the reaction was complete, the mixture was washed sequentially with aqueous saturated NaHCO₃ solution and dilute hydrochloric acid. The organic layer was separated and then dried over anhydrous MgSO₄. After removal of the solvent, the residue obtained was purified by flash column chromatography to afford the pure product.

Coupling of *N*-Deprotected Aminoxy Acid (or Oligopeptide) with Pivaloyl Chloride¹¹. The *N*-deprotected aminoxy acid (or oligopeptide) (0.8 mmol) was dissolved in CH₂Cl₂ (5 mL). Another 5 mL of 5% aqueous NaHCO₃ solution (or pyridine, 1.9 mmol) was added. The mixture was vigorously stirred while pivaloyl chloride (0.20 mL, 1.60 mmol) was added dropwise at 0 °C. The resulting mixture was stirred overnight at room temperature and diluted with CH₂Cl₂ (50 mL). This organic solution was washed with brine and dried over anhydrous MgSO₄. After removal of the solvent, the residue obtained was purified by flash column chromatography to afford the pure product.

Coupling of *C*-Deprotected Aminoxy Acid (or Oligopeptide) with Isobutylamine^{10b}. Isobutylamine (1.73 mmol) was added to a solution of *C*-deprotected aminoxy acid (or oligopeptide) (1.73 mmol) in CH₂Cl₂ (10 mL). To this mixture were added HOAt (354 mg, 2.60 mmol) and EDCI (668 mg, 2.25 mmol). The reaction mixture was stirred overnight. When the reaction was completed, the mixture was washed sequentially with aqueous saturated NaHCO₃ solution and dilute hydrochloric acid. It was then dried over anhydrous MgSO₄. After removal of the solvent, the residue obtained was purified by flash column chromatography to afford the pure product.

Coupling of *N*-Deprotected Aminoxy Acid (or Oligopeptide) with *C*-Deprotected Aminoxy Acid (or Oligopeptide)¹¹. *N*-Deprotected aminoxy acid (or oligopeptide) (2 mmol) was added to the solution of *C*-deprotected aminoxy acid (2 mmol) in CH₂Cl₂ (10 mL). To this mixture were added HOAt (362 mg, 2.66 mmol) and EDCI (772 mg, 2.60 mmol). The reaction mixture was stirred overnight. When the reaction was completed, the mixture

was washed sequentially with aqueous saturated NaHCO₃ solution and dilute hydrochloric acid. It was then dried over anhydrous MgSO₄. After removal of the solvent, the residue obtained was purified by flash column chromatography to afford the pure product.

Characterization Data of Compounds 1–9. Piv-OAcc-NHⁱBu (1): white solid; mp 100–101 °C; *R*_f = 0.3 (EtOAc/hexane = 1:1); ¹H NMR (400 MHz, CDCl₃) δ 8.74 (br, 1H), 8.47 (br, s, 1H), 3.10 (dd, *J* = 6.4, 6.2 Hz, 2H), 1.84–1.79 (m, 1H), 1.43–1.41 (m, 2H), 1.23–1.20 (m, 11H), 0.92 (d, *J* = 6.7 Hz, 6H); ¹³C NMR (100 MHz, CDCl₃) δ 178.7, 170.6, 68.0, 47.4, 38.3, 28.5, 27.2, 20.3, 15.4; IR (CH₂Cl₂) 3250, 3097, 1674 cm⁻¹; EI-MS (20 eV) *m/z* 156 (100), 256 (M⁺, 3); HRMS-EI *m/z* for C₁₃H₂₄N₂O₃ (M⁺) calcd 256.1787, found 256.1793.

ⁱPrCO-D-OVal-OAcc-NHⁱBu (2): white solid; mp 132–133 °C; *R*_f = 0.5 (acetone in CH₂Cl₂ = 5%); [α]_D²⁰ +44.5 (c 1.0, CHCl₃); ¹H NMR (400 MHz, CDCl₃) δ 11.89 (s, 1H), 8.51 (br, s, 1H), 8.43 (s, 1H), 4.08 (d, *J* = 3.2 Hz, 1H), 3.16–2.96 (m, 2H), 2.34–2.25 (m, 2H), 1.85–1.78 (m, 1H), 1.55–1.33 (m, 4H), 1.18 (d, *J* = 6.9 Hz, 3H), 1.17 (d, *J* = 6.9 Hz, 3H), 1.08 (d, *J* = 6.9 Hz, 3H), 0.95–0.91 (m, 9H); ¹³C NMR (100 MHz, CDCl₃) δ 178.5, 171.0, 169.6, 91.5, 68.0, 47.4, 32.4, 30.7, 28.6, 20.3, 19.3, 19.1 (2), 16.9, 16.1 (14, 9); IR (CH₂Cl₂) 3263, 1675, 1640 cm⁻¹; EI-MS (20 eV) *m/z* 130 (100), 357 (M⁺, 3); HRMS (EI) *m/z* for C₁₇H₃₁N₃O₅ (M⁺) calcd 357.2264, found 357.2261.

Piv-OAcc-D-OVal-NHⁱBu (3): colorless oil; *R*_f = 0.5 (acetone in CH₂Cl₂ = 10%); [α]_D²⁰ +28.8 (c 1.0, CHCl₃); ¹H NMR (400 MHz, CDCl₃) δ 12.13 (s, 1H), 8.35 (s, 1H), 8.24 (br, s, 1H), 4.08 (d, *J* = 3.2 Hz, 1H), 3.18–2.99 (m, 2H), 2.36–2.33 (m, 1H), 1.84–1.77 (m, 1H), 1.46–1.27 (m, 4H), 1.22 (s, 9H), 1.17 (d, *J* = 7.3 Hz, 3H), 0.95 (d, *J* = 7.3 Hz, 3H), 0.92–0.90 (m, 6H); ¹³C NMR (100 MHz, CDCl₃) δ 179.8, 170.6, 169.9, 91.6, 67.8, 46.6, 38.4, 30.7, 28.5, 27.1, 20.3(2), 19.3, 16.9, 16.2, 15.6; IR (CH₂Cl₂) 3246, 2964, 1651 cm⁻¹; EI-MS (20 eV) *m/z* 131 (100), 371 (M⁺, 3); HRMS (EI) *m/z* for C₁₈H₃₃N₃O₅ (M⁺) calcd 371.2420, found 371.2401.

Piv-D-OLeu-OGly-NHⁱBu (4): yellow oil; [α]_D²⁰ +60.8 (c 1.0, CH₃CH₂OH); ¹H NMR (400 MHz, CDCl₃) δ 12.05 (s, 1H), 9.40 (s, 1H), 8.35 (s, 1H), 4.42–4.29 (m, 3H), 3.10–3.13 (m, 2H), 1.66–1.89 (m, 4H), 1.21 (s, 9H), 0.97–0.92 (m, 12H); ¹³C NMR (100 MHz, CDCl₃) δ 180.0, 171.8, 167.2, 85.6, 76.0, 46.6, 41.0, 28.3, 27.1, 24.6, 23.2, 21.7, 20.2; IR (CH₂Cl₂) 3380, 3162, 1677 cm⁻¹; ESI-MS, *m/z* 360 (M⁺ + 1, 100); HRMS (EI) for C₁₇H₃₃N₃O₅ (M⁺) calcd 359.2420, found 359.2416.

Piv-OGly-D-OLeu-NHⁱBu (5): white solid; mp 91–93 °C; [α]_D²⁰ +54.9 (c 1.00, CH₃CH₂OH); ¹H NMR (300 MHz, CDCl₃) δ 12.09 (s, br, 1H), 9.57 (s, br, 1H), 8.05 (s, br, 1H), 4.39 (AB, *J* = 16.3 Hz, 2H), 4.31 (dd, *J* = 8.9, 6.6 Hz, 1H), 3.13–3.02 (m, 2H), 1.95–1.67 (m, 4H), 1.21 (s, 9H), 1.03–0.90 (m, 12H); ¹³C NMR (75 MHz, CDCl₃) δ 180.2, 172.0, 167.6, 86.2, 76.2, 47.0, 41.2, 28.8, 27.4, 25.2, 23.6, 22.0, 20.5; IR (CH₂Cl₂) 3380, 3168, 1673, 1605 cm⁻¹; ESI-MS *m/z* 360 (M⁺ + 1, 100); HRMS (EI) for C₁₇H₃₃N₃O₅ (M⁺) calcd 359.2420, found 359.2408.

ⁱPrCO-D-OLeu-(OAcc)₂-NHⁱBu (6): colorless oil; *R*_f = 0.5 (acetone in CH₂Cl₂ = 10%); [α]_D²⁰ +133.1 (c 1.0, CHCl₃); ¹H NMR (400 MHz, CDCl₃) δ 12.10 (s, 1H), 11.98 (s, 1H), 8.67 (s, 1H), 8.62 (br, s, 1H), 4.31 (dd, *J* = 8.2, 5.0 Hz, 1H), 3.10–3.07 (m, 2H), 2.36–2.29 (m, 1H), 1.81–1.69 (m, 4H), 1.60–1.42 (m, 8H), 1.18 (d, *J* = 6.0 Hz, 3H), 1.16 (d, *J* = 6.4 Hz, 3H), 0.98–0.95 (m, 6H), 0.90 (d, *J* = 6.9 Hz, 6H); ¹³C NMR (100 MHz, CDCl₃) δ 178.9, 171.7, 170.8, 170.1, 85.5, 68.0, 67.6, 47.4, 40.7, 32.4, 28.4, 24.6, 23.3, 21.6, 20.3, 19.3, 19.1, 17.3, 16.1, 16.0, 15.7; IR (CH₂Cl₂) 3293, 3149, 1654 cm⁻¹; EI-MS (20 eV) *m/z* 145 (100), 471 (M⁺, 3); HRMS (EI) *m/z* for C₂₂H₃₈N₄O₇ (M⁺) calcd 470.2740, found 470.2724.

Piv-D-OLeu-(OAcc)₃-NHⁱBu (7): colorless oil; *R*_f = 0.4 (acetone in CH₂Cl₂ = 10%); [α]_D²⁰ +54.2 (c 1.0, CHCl₃); ¹H

NMR (400 MHz, CDCl₃) δ 12.21 (s, 1H), 12.18 (s, 1H), 12.17 (s, 1H), 8.58 (t, *J* = 5.5, 1H), 8.53 (s, 1H), 4.30 (dd, *J* = 6.8, 6.4 Hz, 1H), 3.08 (t, *J* = 6.4 Hz, 2H), 1.86–1.70 (m, 4H), 1.52–1.32 (m, 12H), 1.22 (s, 9H), 0.99–0.96 (m, 6H), 0.90 (d, *J* = 6.9 Hz, 6H); ¹³C NMR (100 MHz, CDCl₃) δ 180.4, 171.7, 171.4, 170.8, 169.9, 85.4, 68.0, 67.6, 67.5, 47.3, 40.7, 38.2, 28.4, 27.0, 24.6, 23.1, 21.7, 20.2, 17.6, 16.6, 16.5(2), 15.7, 15.6; IR (CH₂Cl₂) 3432, 3220, 1645 cm⁻¹; EI-MS (20 eV) *m/z* 145 (100), 583 (M⁺, 3); HRMS (EI) *m/z* for C₂₇H₄₅N₅O₉ (M⁺) calcd 583.3217, found 583.3178.

¹PrCO-D-OVal-OAcc-D-OVal-NH^tBu (8): white solid; mp 199–201 °C; *R_f* = 0.5 (acetone in CH₂Cl₂ = 10%); [α]_D²⁰ +82.4 (*c* 1.0, CHCl₃); ¹H NMR (400 MHz, CDCl₃) δ 12.11 (s, 1H), 11.93 (s, 1H), 8.43 (s, 1H), 8.39 (br, s, 1H), 4.13 (d, *J* = 3.8 Hz, 2H), 3.19–2.96 (m, 2H), 2.36–2.30 (m, 3H), 1.82–1.77 (m, 1H), 1.50–1.33 (m, 4H), 1.25–1.05 (m, 12H), 0.96–0.88 (m, 12H); ¹³C NMR (100 MHz, CDCl₃) δ 178.9, 171.3(2), 170.9, 91.8, 91.6, 68.0, 47.1, 32.5, 31.2, 31.0, 28.7, 20.5(2), 19.7, 19.6, 19.4, 19.2, 18.2, 16.6, 16.4, 15.4; IR (CH₂Cl₂) 3427, 3206, 1680, 1648 cm⁻¹; EI-MS (20 eV) *m/z* 130 (100), 472 (M⁺, 33); HRMS (EI) *m/z* for C₂₂H₄₀N₄O₇ (M⁺) calcd 472.2897, found 472.2890.

¹PrCO-(D-OVal-OAcc)₂-D-OVal-NH^tBu (9): colorless oil; *R_f* = 0.4 (acetone in CH₂Cl₂ = 10%); [α]_D²⁰ +125.3 (*c* 1.0, CHCl₃); ¹H NMR (400 MHz, CDCl₃) δ 12.42 (s, 1H), 12.36 (s, 2H), 12.10 (s, 1H), 9.42 (s, 1H), 8.47 (br, s, 1H), 4.22 (d, *J* = 3.7 Hz, 1H), 4.10 (br, s, 2H), 3.15–2.98 (m, 2H), 2.34–2.31 (m, 4H), 1.83–1.07

(m, 21H), 0.94–0.87 (m, 18H); ¹³C NMR (100 MHz, CDCl₃) δ 178.9, 172.2, 171.1, 171.0, 170.9, 170.4, 91.5 (3), 67.6, 67.5, 46.7, 32.4, 30.9, 30.8, 30.7, 28.4, 20.3, 20.2, 19.4, 19.3, 19.1, 18.9, 18.8, 18.3, 17.8, 16.2, 16.1, 15.9, 15.5, 15.0; IR (CH₂Cl₂) 3160, 2966, 1671 cm⁻¹; EI-MS (20 eV) *m/z* 130 (100), 686 (M⁺, 15); HRMS (EI) *m/z* for C₃₁H₅₄N₆O₁₁ (M⁺) calcd 686.3851, found 686.3854.

Acknowledgment. This work was supported by Fudan University, the National Natural Science Foundation of China (Project No. 20202001), the Fok Ying Tung Education Foundation (Project No. 94023), the HKU-Fudan Joint Laboratory on Molecular Design and Synthesis, and the Research Grants Council of Hong Kong (Project Nos. HKU 7654/06M and HKU 2/06C). D.-W.Z. thanks Fudan University for the conferment of the Century Star Award.

Supporting Information Available: Synthetic schemes and characterization data of synthetic intermediates **10–22**; ¹H NMR experimental results of compound **1**; calculated structures of models **III** and **IV** optimized by using B3LYP/6-31(d,p); CD spectra of oligopeptides **2–9**; data for the crystals of compounds **1**, **2**, and **8**. This material is available free of charge via the Internet at <http://pubs.acs.org>.